Heat-Exchanger Network Design for the Atmospheric Distillation Unit at Zawiya Refinery: A Comparison of Pinch Analysis and a Simplified Superstructure Approach

Areej Masoud Ali[(1)], Rabeeah Husayn Sultan Husayn[(2)], Najib Meftah Almukhtar Omar[(3)], Abduelaged Al-Bashir Abduallah[(4)].

[(1) (2) (3) (4)]Chemical Engineering Department, Sabratha Faculty of Engineering, Sabratha University Libya

areej.ali@sabu.edu.ly , rabeaa.huseen@sabu.edu.ly , najib.omar@sabu.edu.ly .

ABSTRACT

The heat-exchanger network (HEN) of the crude-oil atmospheric distillation unit at Zawiya Refinery, Libya, has received little systematic attention despite several decades of operation. This study compares a pinch-based design with a simplified superstructure approach applied to the same nine-stream data set (six hot and three cold streams). A minimum approach temperature of ΔT_{min} = 20 °C, identified from the total annual cost (TAC) curve generated with HINT software, gives minimum hot- and cold-utility targets of 23,457.156 kW and 10,882.814 kW, respectively, with pinch temperatures of 126 °C (hot) and 106 °C (cold). Shell targeting on the balanced composite curves, with each 1–2 shell limited to 85% of its maximum thermal effectiveness, gives a target of 29 shells (13 below and 16 above the pinch). The pinch-based network comprises nine process exchangers, one heater and four coolers (14 units), which equals the minimum number of units required for maximum energy recovery. The simplified superstructure, constructed by partitioning the balanced composite curves into eight enthalpy intervals, requires 34 shells before exchanger integration, and its integrated network contains 18 units. Pinch analysis therefore supplies the energy targets and the design constraints, whereas the interval-based superstructure supplies a systematic route to network construction. The hot-utility target is 374 kW (1.6%) below the value reported previously for the same unit; because the cold-utility targets agree, this points to differences in the stream data or net heat balance rather than in ΔT_{min}. Because capital-cost, heat-transfer-area and operability data are not available for both networks, no economic ranking is attempted.

Received: 26-07-2026 Accepted: 18-08-2026 Published: 02-09-2026

Keywords: Heat-exchanger network, Pinch analysis, Superstructure, Crude-oil distillation, Energy integration

1. Introduction

Atmospheric distillation is the first separation step in a petroleum refinery and one of its most energy-intensive operations. The crude-preheat train, which recovers heat from product and pump-around streams, largely determines the duty of the fired heater and therefore the fuel consumption and carbon emissions of the unit. The crude-oil atmospheric distillation unit at Zawiya Refinery has operated for several decades, yet its heat-exchanger network (HEN) has received limited attention in the published literature. An early study applied the temperature-interval method to an existing crude-distillation unit and concluded that practically and economically viable crude-preheat recovery was limited to approximately 14 MMBtu h^{-1} (≈4.1 MW) [1]. A subsequent study applied pinch technology to the refinery's crude-distillation heat-exchanger train and estimated that the proposed network could reduce fuel consumption by approximately 20% [2].

Rahouma et al. [3] investigated HEN optimisation for the same crude-distillation unit using pinch analysis. They reported an optimum ΔT_{min} of 20 °C, minimum hot- and cold-utility requirements of 23,831.5 kW and 10,882.8 kW, an estimated annual operating cost of USD 2.97 million and a total heat-transfer area of 14,507.48 m^2. The hot-utility target obtained in the present study (23,457.156 kW) differs from the value of Rahouma et al. [3], whereas the cold-utility targets are nearly identical at the reported precision.

HEN synthesis has been reviewed extensively [4,5] and has been approached through pinch analysis [6–9], mathematical programming, including transhipment and superstructure models [10,11], stochastic and evolutionary optimisation [12,13], thermodynamic design methods [14] and systematic retrofit procedures [15]. Pinch analysis establishes thermodynamic energy targets and provides design rules for matching streams above and below the pinch. Superstructure methods, in contrast, embed alternative heat-exchange matches within a defined network structure and provide a systematic framework for generating and evaluating candidate configurations. The two families of methods are complementary: energy targeting constrains the design space, while network-synthesis procedures support the construction and evaluation of feasible exchanger arrangements. A comparison between design routes is meaningful, however, only if utility targets, shell counts

and equipment-unit counts are reported on a consistent basis, because these quantities measure different things.

The objectives of this study are therefore to (i) establish the energy targets for the Zawiya crude-distillation unit at a TAC-based ΔT_{min}. (ii) derive a shell target from the balanced composite curves. (iii) develop a pinch-based network and a simplified superstructure network for the same stream data. (iv) compare the two on a consistent accounting basis that separates shell counts from equipment-unit counts. The contribution is a comparative, case-specific application with explicit accounting rather than a claim that the simplified superstructure procedure is a new general optimisation algorithm. An economic or operational ranking is not attempted because equivalent capital-cost, operating-cost, heat-transfer-area and operability data are not available for both networks.

2. Process description and stream data

2.1. Process description

The atmospheric distillation unit (Unit 10) comprises a crude-oil heat-recovery train, a desalter, a fired heater and the main atmospheric column V-1 (Fig. 1). The crude feed is preheated in two stages separated by desalting, heated further in the fired heater (tag H-1, not to be confused with hot stream H-1 in Table 1) and introduced into the flash zone of column V-1, where it is separated into product fractions. In the first preheat stage, upstream of desalter V-3, the crude recovers heat from process streams that include the top pump-around (TPA), heavy gas oil (HGO) and atmospheric residue (RS). After desalting, the crude is pumped through the second preheat stage, where it exchanges heat with additional process streams, including light gas oil (LGO), kerosene and pump-around streams. Atmospheric residue is withdrawn from the column bottom, heavy gas oil from an intermediate section and naphtha from the overhead system.

The TPA is withdrawn near tray 5, exchanges heat with the crude feed in exchanger E1 and is returned to the column. The bottom pump-around (BPA) is withdrawn near tray 18, exchanges heat with the crude feed in exchanger E4 and is then returned to the column; it enters at 261 °C and leaves at 192 °C, which corresponds to stream H-3 in Table 1.

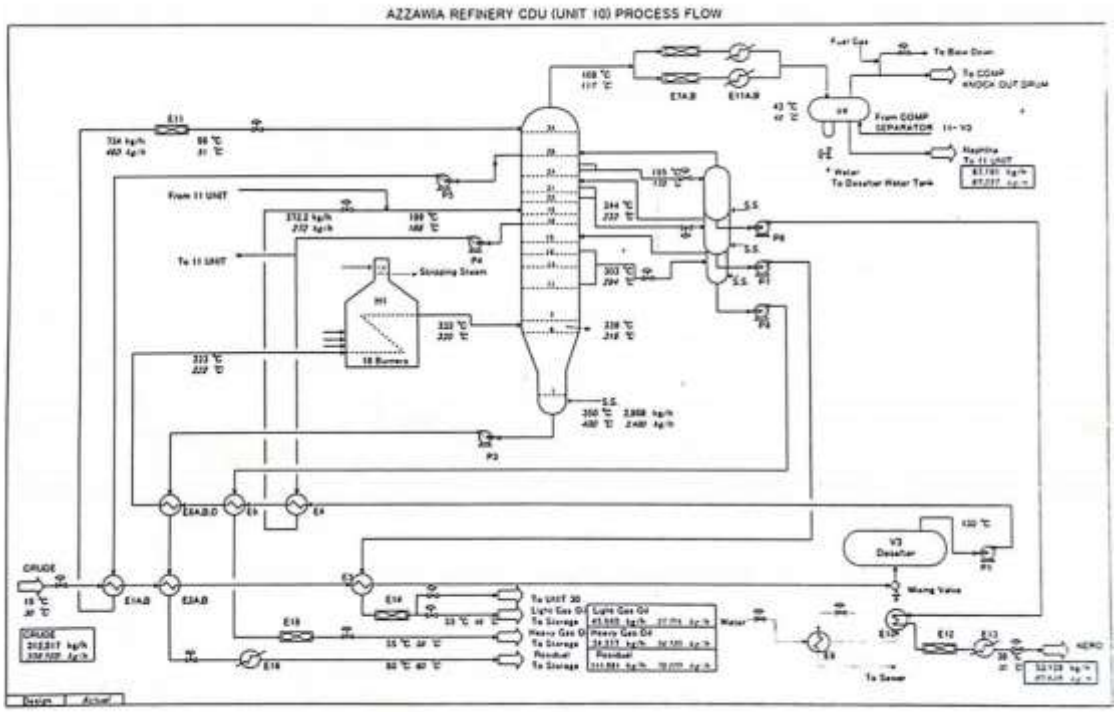


Figure 1. Process-flow diagram of the crude-oil atmospheric distillation unit (Unit 10) at Zawiya Refinery, showing the principal process sections and the heat-recovery context.

2.2. Stream data and energy balance

The supply and target temperatures, heat-capacity flow rates and enthalpy changes used in the HEN analysis are listed in Table 1. The data set comprises six hot streams (H-1 to H-6) and three cold streams (C-1 to C-3). Enthalpy changes are tabulated as magnitudes; the hot/cold classification, rather than the sign, identifies the direction of heat transfer.

Table 1. Process-stream thermal data for the Zawiya crude-oil atmospheric distillation unit: supply temperature (Ts), target temperature (Tt), heat-capacity flow rate (CP) and enthalpy-change magnitude (ΔH).

Stream	Type	T_s (°C)	T_t (°C)	CP (kW/°C)	$\lvert\Delta H\rvert$ (kW)
H-1	Hot	319	80	68.711	16,421.929
H-2	Hot	298	47	27.347	6,864.097
H-3	Hot	261	192	95.130	6,563.970

Stream	Type	T_s (°C)	T_t (°C)	CP (kW/°C)	$\|\Delta H\|$ (kW)
H-4	Hot	231	47	34.421	6,333.464
H-5	Hot	173	34	41.290	5,739.310
H-6	Hot	126	53	229.595	16,760.435
C-1	Cold	20	116	201.126	19,308.090
C-2	Cold	116	332	238.563	51,529.600
C-3	Cold	80	99	22.097	419.843

From the listed values, the six hot streams release 58,683.205 kW, and the three cold streams require 71,257.533 kW, giving a net process heat deficit of 12,574.328 kW. The utility targets reported in Section 4.1 satisfy $Q_{H,min} - Q_{C,min} = 12{,}574.342$ kW, which differs from the stream-data balance by 0.014 kW (about 10^{-4}%). This residual is consistent with rounding in the displayed cold-stream heat-capacity flow rates: the products $C_P|T_s - T_t|$ reproduce the hot-stream enthalpy changes exactly, differ from the tabulated values by 0.006 kW (C-1) and 0.008 kW (C-2), and agree for C-3.

3. Methodology

3.1. Selection of the minimum temperature difference

The minimum temperature difference, ΔT_{min}, is a key design parameter because it governs the trade-off between process heat recovery and heat-transfer area. A smaller ΔT_{min} permits greater process-to-process heat recovery but requires larger heat-transfer surfaces and may increase capital cost; a larger ΔT_{min} reduces the required area but increases external utility demand. HINT software was used to evaluate the total annual cost (TAC) over a ΔT_{min} range of 5–50 °C, with 20–40 °C taken as the initial practical range. The cost parameters embedded in the TAC calculation (annualisation period, utility prices, exchanger-area cost correlation, installation factors and operating hours) are not itemised in the source data set.

3.2. Balanced composite curves and shell targeting

The balanced hot and cold composite curves (BHCC and BCCC) include the hot and cold utilities, so that the total enthalpy released by the hot side equals the total enthalpy absorbed by the cold side at every point. Hot

and cold temperatures that share the same cumulative enthalpy define a set of 20 composite-curve segments (i = 1–20), each bounded by two successive enthalpy levels. These segments are used for shell targeting and are distinct from the eight enthalpy intervals of the superstructure procedure (Section 3.4).

For a multipass shell-and-tube exchanger, the heat-transfer relation is

$$Q = U A F_T \Delta T_{LM} \tag{1}$$

where Q is the heat duty, U the overall heat-transfer coefficient, A the heat-transfer area, F_T the correction factor for departure from counter-current flow, and ΔT_{LM} the counter-current log-mean temperature difference. F_T depends on the dimensionless parameters P (thermal effectiveness) and R (heat-capacity ratio). For segment i, with $T_{h,i}$ and $T_{c,i}$ the hot and cold temperatures at its upper boundary and $T_{h,i-1}$ and $T_{c,i-1}$ those at its lower boundary, the parameters are

$$P_i = (T_{h,i} - T_{h,i-1}) / (T_{h,i} - T_{c,i-1}) \tag{2}$$

$$R_i = (T_{c,i} - T_{c,i-1}) / (T_{h,i} - T_{h,i-1}) \tag{3}$$

The number of transfer units required for counter-current operation is

$$NTU_{cf}(P, R) = \ln[(1 - P) / (1 - RP)] / (R - 1) \tag{4}$$

with $NTU_{cf} = -\ln(1 - P)$ for R = 0. For a single 1–2 shell, the maximum attainable effectiveness at a given R is

$$P_{max,i} = 2 / [R_i + 1 + \sqrt{(R_i^2 + 1)}] \tag{5}$$

In this study, each shell is loaded to 85% of this maximum,

$$P_{12,i} = 0.85\, P_{max,i} \tag{6}$$

which keeps the correction factor above the acceptance criterion $F_T > 0.8$. Evaluated with the standard 1–2 expression for F_T, the loading in Eq. (6) gives F_T between 0.806 and 1.000 for the R_i values of the present data

set. The number of shells associated with segment i is then the ratio of the counter-current NTU required to that delivered by one shell at $P_{12,i}$,

$$N_i = \mathrm{NTU}_{cf}(P_i, R_i) / \mathrm{NTU}_{cf}(P_{12,i}, R_i) \quad (7)$$

and the shell contribution of the segment is

$$N_{s,i} = N_i (S_i - 1) \quad (8)$$

where S_i is the number of streams, including utilities, present in segment i, so that $S_i - 1$ is the number of exchangers needed to satisfy the segment. The segment contributions are summed separately below and above the pinch, and each subtotal is rounded upward, because no exchanger shell can straddle the pinch:

$$N_s = \lceil \Sigma N_{s,i} \rceil_{\mathrm{below}} + \lceil \Sigma N_{s,i} \rceil_{\mathrm{above}} \quad (9)$$

Equations (2)–(8) were verified against the tabulated P_i, R_i, $P_{max,i}$, $P_{12,i}$, N_i and $N_{s,i}$ values reported in Section 4.2, which they reproduce to the displayed precision. The shell-targeting concept on balanced composite curves was introduced by Ahmad et al. [16]; the effectiveness-based formulation above is the implementation used here, and the factor 0.85 is an adopted design choice rather than a derived quantity.

3.3. Pinch design method

The pinch-based network was developed using HINT software and the standard pinch design method [7–9]. Three rules govern the design: (i) no heat is transferred across the pinch; (ii) no external cooling is used above the pinch; and (iii) no external heating is used below the pinch. Any violation of these rules introduces cross-pinch heat transfer and increases external utility demand relative to the thermodynamic target. The network is therefore designed independently above and below the pinch, and every match must satisfy the specified minimum approach temperature. Candidate matches were screened against three feasibility criteria: the heat-

capacity-flow-rate criterion at the pinch, the stream-count criterion, and the heat-capacity-flow-rate-difference criterion used to rank competing matches.

For a network without loops, Euler's theorem gives the minimum number of units for maximum energy recovery as

$$U_{min,MER} = (N_{above} - 1) + (N_{below} - 1) \quad (10)$$

where N_{above} and N_{below} are the numbers of streams, including utilities, present above and below the pinch. Equation (10) serves as the benchmark for the equipment-unit count of each network developed here.

3.4. Simplified superstructure procedure

The simplified superstructure procedure divides the balanced composite curves, including utility contributions, into sections. Each section is treated as a subnetwork in which candidate stream matches are evaluated using local temperatures and enthalpy balances. The term "enthalpy interval" denotes each region between adjacent boundaries on the enthalpy coordinate of the balanced composite curves. The construction proceeds as follows:

1. Draw a horizontal line from the highest cold-composite-curve temperature to its intersection with the hot composite curve.
2. From this intersection, draw a vertical line to the cold composite curve.
3. Repeat the construction until the horizontal boundary reaches the left-hand enthalpy ordinate.
4. Treat the regions between adjacent vertical boundaries as separate enthalpy intervals.
5. Determine the hot- and cold-stream temperatures and enthalpy changes within each interval.
6. Check the enthalpy balance and confirm that the hot-stream temperature is not lower than the corresponding cold-stream temperature at the relevant match points.
7. Develop a feasible subnetwork for each interval while maintaining the pinch-design rules.
8. Where an exchanger loop is identified, assess loop breaking or exchanger integration to determine whether the network can be simplified without violating ΔT_{min} or temperature-crossing constraints.

4. Results and discussion

4.1. Optimum ΔT_{min} and utility targets

The TAC curve calculated with HINT reaches its minimum at approximately ΔT_{min} = 20 °C (Fig. 2), which is therefore adopted for the pinch-based and superstructure designs. A lower ΔT_{min} increases process heat recovery at the cost of larger exchanger area, whereas a higher value reduces area but raises utility consumption; the TAC curve resolves this trade-off at 20 °C within the cost model embedded in the software (Section 3.1). Because the economic assumptions behind the curve are not itemised, the value is treated as the reported optimum rather than as an independently validated one.

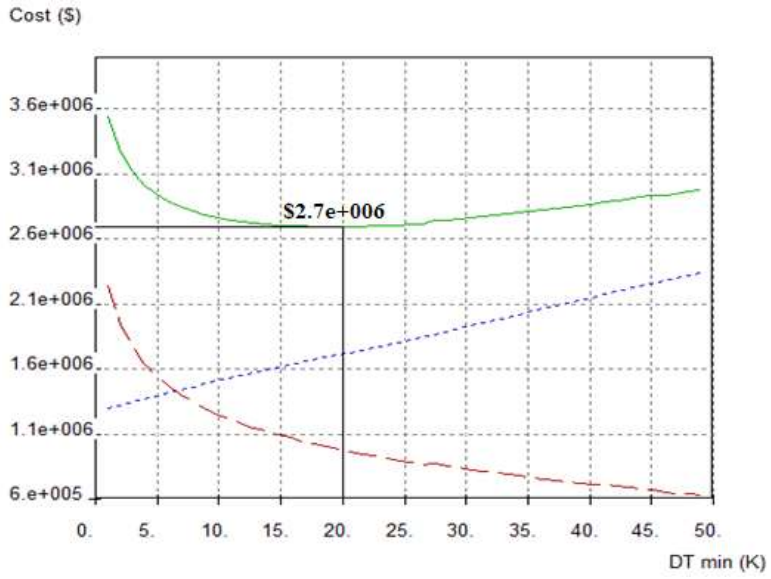


Figure 2. Total annual cost (TAC) as a function of the minimum temperature difference (ΔT_{min}), calculated using HINT software.

Figure 3 shows the minimum hot- and cold-utility targets as functions of ΔT_{min}. At ΔT_{min} = 20 °C, the targets are $Q_{H,min}$ = 23,457.156 kW and $Q_{C,min}$ = 10,882.814 kW. Of the 58,683.205 kW released by the hot streams, at most 47,800.391 kW (81.5%) can be transferred to the cold streams, which meets 67.1% of the 71,257.533 kW cold-stream demand; the remaining 32.9% must be supplied by the hot utility (Table 2).

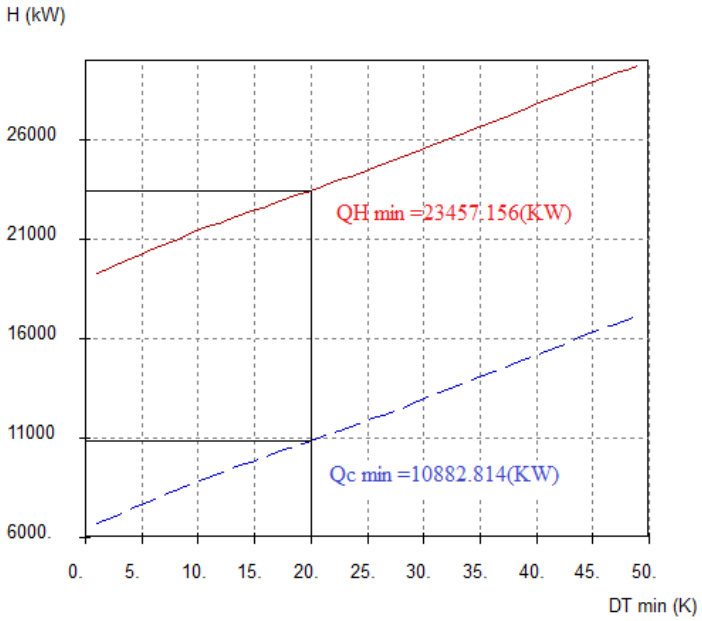


Figure 3. Minimum hot- and cold-utility targets ($Q_{H,min}$ and $Q_{C,min}$) as functions of ΔT_{min} for the crude-oil atmospheric distillation-unit HEN.

Table 2. Energy and unit targets at ΔT_{min} = 20 °C.

Quantity	Value
Minimum temperature difference, ΔT_{min}	20 °C
Pinch temperature (hot/cold)	126 °C / 106 °C
Minimum hot-utility target, $Q_{H,min}$	23,457.156 kW
Minimum cold-utility target, $Q_{C,min}$	10,882.814 kW
Total hot-stream duty / total cold-stream duty	58,683.205 kW / 71,257.533 kW
Maximum process-to-process heat recovery[a]	47,800.391 kW (81.5% of hot-stream duty; 67.1% of cold-stream duty)
Minimum number of units for maximum energy recovery, $U_{min,MER}$[b]	14 (7 above + 7 below the pinch)
Shell target, N_s	29 (13 below + 16 above the pinch)

[a] Total hot-stream duty minus $Q_{C,min}$. [b] Eq. (10) with N_{above} = 8 (hot streams H-1 to H-5, cold streams C-1 and C-2, hot utility) and N_{below} = 8 (hot streams H-1, H-2, H-4, H-5 and H-6, cold streams C-1 and C-3, cold utility).

The hot-utility target is 374.3 kW (1.6%) lower than the 23,831.5 kW reported by Rahouma et al. [3], while the cold-utility targets agree (10,882.814 versus 10,882.8 kW). For any single stream data set, the difference $Q_{H,min} - Q_{C,min}$ must equal the net heat deficit of the streams, independently of ΔT_{min}. The values of Rahouma et al. [3] imply a net deficit of 12,948.7 kW, which exceeds the present value of 12,574.3 kW by 374.4 kW (3.0%). Because the cold-utility targets coincide, the discrepancy is therefore attributable to a difference in the stream data (for example, in heat-capacity flow rates, temperatures or the number of streams) rather than to the choice of ΔT_{min} or to the targeting algorithm. The two hot-utility values should consequently not be treated as directly comparable until the stream data are aligned.

4.2. Composite curves and shell target

Figure 4 shows the balanced composite curves at ΔT_{min} = 20 °C, with the pinch at 126 °C on the hot curve and 106 °C on the cold curve. Table 3 gives the balanced cold composite-curve data, and Table 4 lists the matched hot and cold temperatures at each cumulative enthalpy level. The pinch lies at a cumulative enthalpy of 28,599.5 kW.

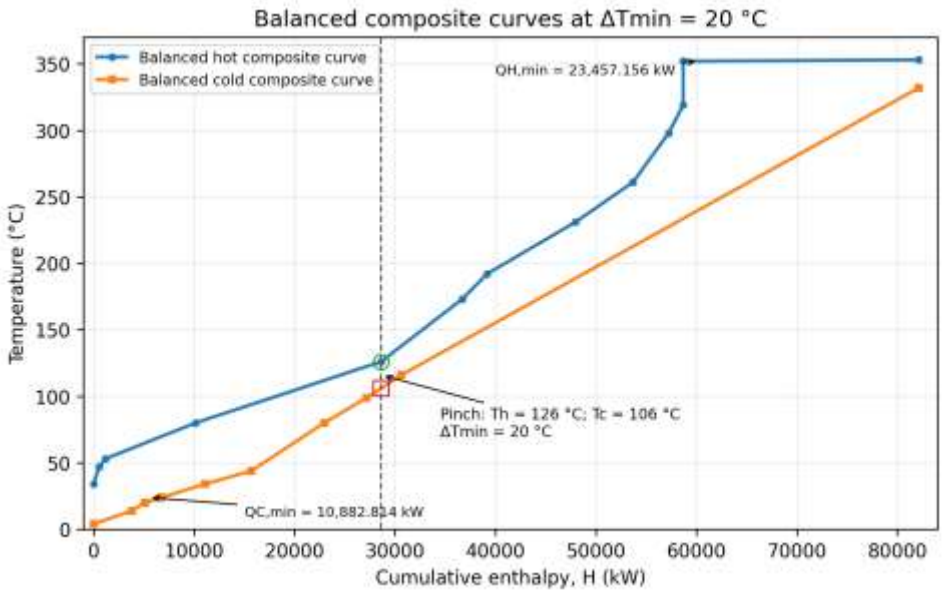


Figure 4. Balanced hot and cold composite curves at ΔT_{min} = 20 °C, showing the pinch temperatures and the utility targets.

Table 3. Balanced cold composite-curve (BCCC) data, including the cold utility. T is the upper temperature of each section; CP is the cold-composite heat-capacity flow rate.

T (°C)	CP (kW °C^{-1})	ΔT (°C)	ΔH (kW)	Cumulative ΔH (kW)
4	—	—	—	0.000
14	379.868	10	3,798.680	3,798.680
20	216.041	6	1,296.246	5,094.926
24	417.167	4	1,668.668	6,763.594
34	431.068	10	4,310.680	11,074.274
44	463.556	10	4,635.560	15,709.834
80	201.126	36	7,240.536	22,950.370
99	223.223	19	4,241.237	27,191.607
116	201.126	17	3,419.142	30,610.749
332	238.563	216	51,529.608	82,140.357

Table 4. Matched temperatures on the balanced hot and cold composite curves at each cumulative enthalpy level (ΔHcum). The pinch is shown in bold.

ΔH_{cum} (kW)	T_h (°C)	T_c (°C)
0	34	4
536.770	47	5.41372
1,155.118	53	7.04230
3,798.680	60.94691	14
5,094.926	64.84680	20
6,763.594	69.86440	24
10,136.749	80	31.82511
11,074.274	82.33585	34
15,709.834	93.88536	44
22,950.370	111.92519	80
27,191.607	122.49225	99
28,599.493	**126**	**106**
30,610.749	137.70907	116
36,672.636	173	141.41000
39,151.737	192	151.80180

ΔH_{cum} (kW)	T_h (°C)	T_c (°C)
47,950.488	231	188.68411
53,686.128	261	212.72656
57,240.274	298	227.62471
58,683.205	319	233.67300
58,683.210	352	233.67300
82,140.360	353	332

The last two hot-side levels (352 and 353 °C) correspond to the hot utility, whose 23,457.156 kW duty is the enthalpy difference between them.

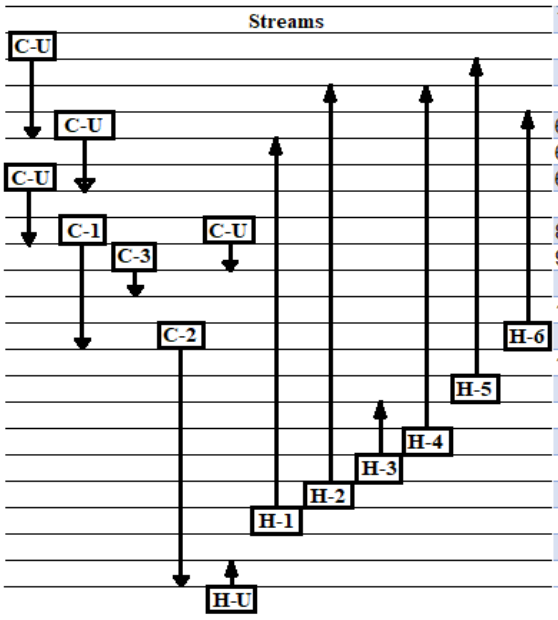
The shell-targeting calculation is summarised in Table 5, and Fig. 5 reproduces the segment-wise worksheet. The below-pinch subtotal (segments 1–11) is 12.5642 shells, and the above-pinch subtotal (segments 12–20) is 15.5455 shells, giving $\Sigma N_{s,i}$ = 28.1097 before rounding, and 13 + 16 = 29 shells after separate upward rounding (Eq. 9). The relative magnitudes of the segment contributions are shown in Fig. 6.

Table 5. Shell-targeting calculation for the 20 composite-curve segments: dimensionless parameters (Eqs. 2, 3, 5, 6), shells per segment (Eq. 7), stream-count factor and shell contribution (Eq. 8).

i	T_h (°C)	P_i	R_i	$P_{max,i}$	$P_{12,i}$	N_i	$S_i - 1$	$N_{s,i}$
1	47	0.3023	0.1087	0.9458	0.8039	0.2124	1	0.2124
2	53	0.1261	0.2714	0.8667	0.7367	0.0899	3	0.2698
3	60.947	0.1474	0.8755	0.6241	0.5305	0.1618	4	0.6473
4	64.847	0.0767	1.5385	0.4573	0.3887	0.1092	4	0.4367
5	69.864	0.1006	0.7972	0.6502	0.5527	0.1004	5	0.5018
6	80	0.1810	0.7720	0.6589	0.5601	0.1929	5	0.9645
7	82.336	0.0462	0.9311	0.6065	0.5155	0.0471	6	0.2828
8	93.885	0.1929	0.8658	0.6272	0.5332	0.2213	6	1.3281
9	111.925	0.2656	1.9956	0.3826	0.3252	0.6830	5	3.4150
10	122.492	0.2487	1.7980	0.4119	0.3501	0.5458	6	3.2745
11	126	0.1299	1.9956	0.3826	0.3252	0.2463	5	1.2314
	Σ below pinch							**12.5642**

i	T_h (°C)	P_i	R_i	$P_{max,i}$	$P_{12,i}$	N_i	$S_i - 1$	$N_{s,i}$
12	137.709	0.3693	0.8540	0.6311	0.5364	0.5254	4	2.1016
13	173	0.6191	0.7200	0.6774	0.5758	1.1644	4	4.6576
14	192	0.3756	0.5469	0.7444	0.6327	0.4177	3	1.2531
15	231	0.4924	0.9457	0.6020	0.5117	0.9276	4	3.7103
16	261	0.4148	0.8014	0.6487	0.5514	0.6030	3	1.8091
17	298	0.4339	0.4027	0.8062	0.6853	0.4524	2	0.9048
18	319	0.2298	0.2880	0.8589	0.7300	0.1795	1	0.1795
19	352	0.2789	0.0000	1.0000	0.8500	0.1723	0	0.0000
20	353	0.0084	98.3270	0.0101	0.0086	0.9295	1	0.9295
	Σ above pinch							**15.5455**
	Σ total							**28.1097**
	Shell target							**29**

Segments 1–11 lie below the pinch and segments 12–20 above it. T_h is the hot-curve temperature at the upper boundary of the segment.



TH	TC	Ni	Si-1	Nsi
34	4			
47	5.41372	0.2123722	1	0.2123722
53	7.042298	0.0899377	3	0.269813
60.946906	14	0.1618368	4	0.6473471
64.846802	20	0.1091729	4	0.4366916
69.864402	24	0.1003526	5	0.5017628
80	31.825111	0.1928942	5	0.9644712
82.335847	34	0.0471341	6	0.2828044
93.885363	44	0.221347	6	1.3280823
111.92519	80	0.6829998	5	3.414999
122.49225	99	0.5457534	6	3.2745206
126	106	0.2462764	5	1.2313821
137.70907	116	0.5254083	4	2.1016331
173	141.41	1.1643935	4	4.6575739
192	151.8018	0.4176973	3	1.253092
231	188.68411	0.9275822	4	3.710329
261	212.72656	0.6030377	3	1.8091132
298	227.62471	0.4523973	2	0.9047946
319	233.673	0.1794748	1	0.1794748
352	233.673	0.172346	0	0
353	332	0.9294946	1	0.9294946
				28.10975

Figure 5. Segment-wise shell-targeting worksheet: stream bars on the balanced composite curves (left) and the corresponding temperatures, N_i, $S_i - 1$ and $N_{s,i}$ (right). The column sum is 28.10975 shells.

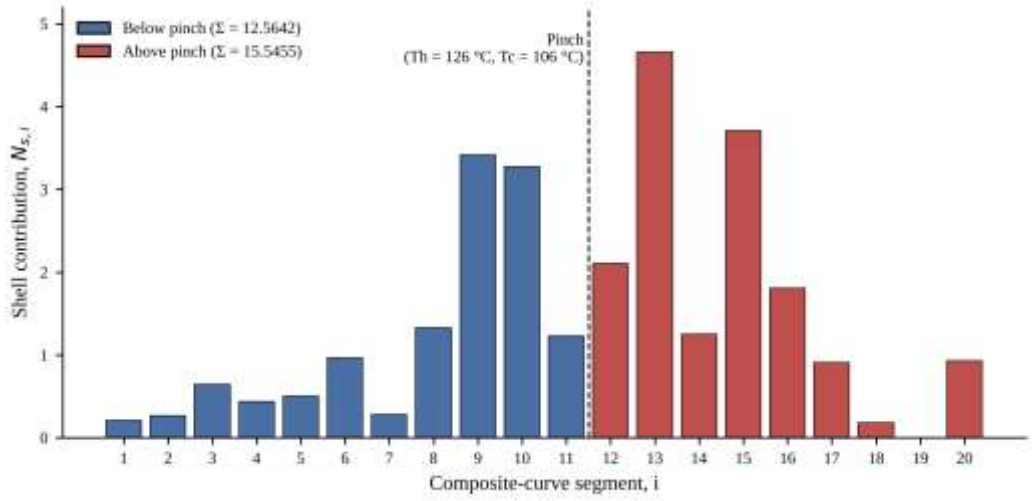


Figure 6. Shell contribution Ns,i of each composite-curve segment from Table 5, shaded by pinch side.

Four segments (i = 9, 10, 13 and 15) account for 15.06 of the 28.11 shells (54%). These segments combine large effectiveness requirements with many streams ($S_i - 1 = 4–6$), which shows that the shell target is driven mainly by the mid-temperature region where several hot streams overlap the cold composite curve. Segments 19 and 20 require separate comment. They correspond to the hot-utility region ($T_h = 352–353$ °C): the utility enters the balanced curve as a stream with a 1 °C temperature span, so that the cold-side range of 98.327 °C yields R = 98.327 and $P_{max} = 0.0101$ for segment 20, while segment 19 has R = 0 and $S_i - 1 = 0$. These unusual values are therefore a consequence of how the utility is represented rather than of a calculation error. Segment 20 nevertheless contributes 0.929 shells (3.3% of the total), so the shell target is mildly sensitive to the utility-temperature convention.

4.3. Pinch-based network

Above the pinch, external cooling is not permitted: heat is recovered by cooling hot process streams against cold process streams, and the hot utility supplies the remaining demand of the cold streams. Figure 7 shows the resulting above-pinch design, with the heater carrying 23,457.1 kW. Below the pinch, external heating is not permitted: cold streams are heated by process-to-process recovery, and cold utility removes the residual heat from the hot streams. Figure 8 shows the below-pinch design. Four coolers remove 2,624.3, 2,160.4, 2,299.4 and 3,798.7 kW from hot streams H-1, H-2, H-4 and H-5, respectively, which sum to 10,882.8 kW, the cold-utility target.

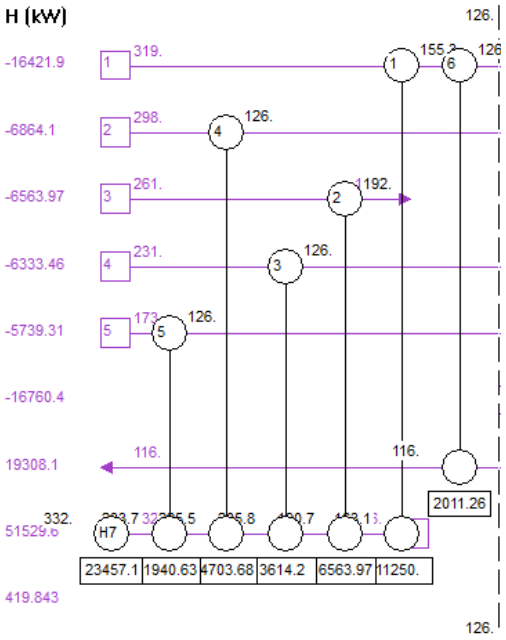


Figure 7. Pinch-based HEN design above the pinch at ΔT_{min} = 20 °C (duties in kW).

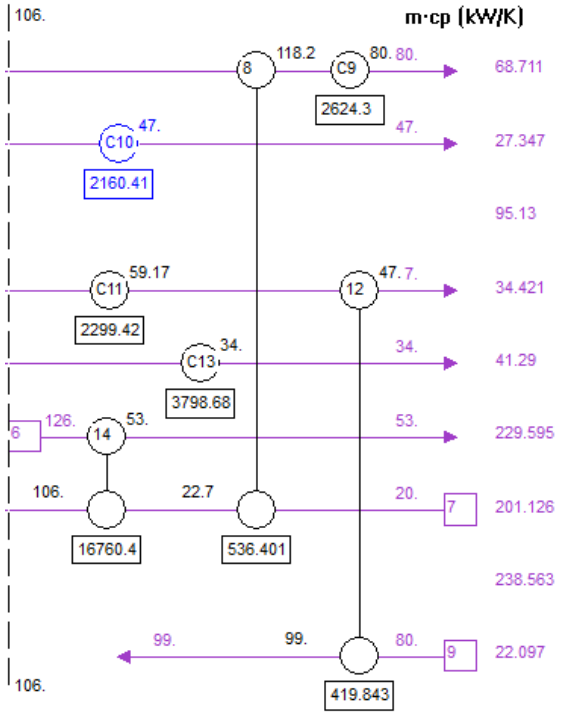


Figure 8. Pinch-based HEN design below the pinch at ΔT_{min} = 20 °C (duties in kW).

The complete pinch-based network (Fig. 9) contains nine process heat exchangers, one heater and four coolers, i.e. 14 equipment units, with seven units above the pinch and seven below it. This equals $U_{min,MER} = 14$ from Eq. (10) (Table 2), so the network attains the minimum number of units for maximum energy recovery and contains no avoidable loops. Its hot- and cold-utility duties equal the targets of 23,457.156 kW and 10,882.814 kW, so no energy penalty is incurred. The 14-unit count is a count of equipment units; it is distinct from the 29-shell target of Section 4.2, and the two are not interchangeable design measures.

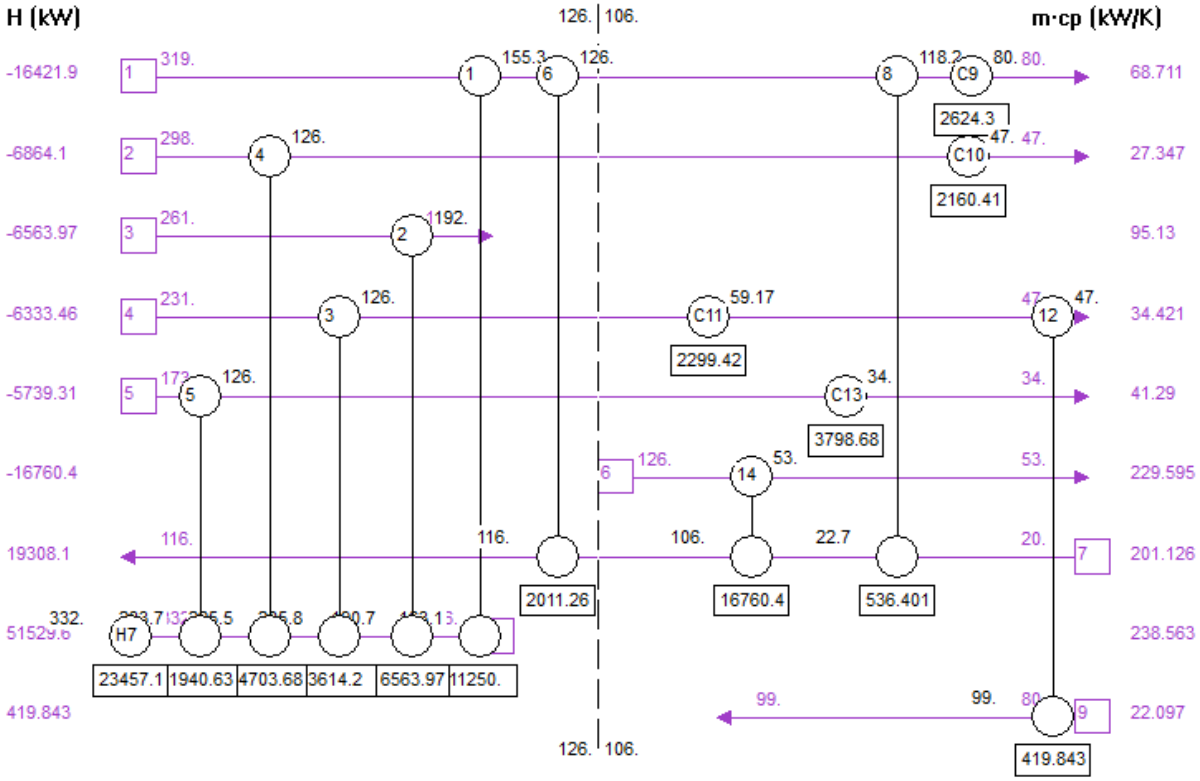


Figure 9. Complete pinch-based HEN obtained by combining the above- and below-pinch designs at $\Delta T_{min} = 20°C$.

4.4. Simplified superstructure network

The balanced composite curves were partitioned into eight enthalpy intervals (Fig. 10), three below the pinch and five above it. Each interval was analysed separately using its local temperature range, heat-transfer duty and utility requirement, which provides a systematic basis for identifying candidate matches. Below the pinch,

process exchangers provide heat recovery, and coolers remove residual heat from the hot streams; above the pinch, process exchangers recover heat, and the heater supplies the remaining cold-stream demand. The simplified superstructure is reported to require 34 shells before exchanger integration (Fig. 11).

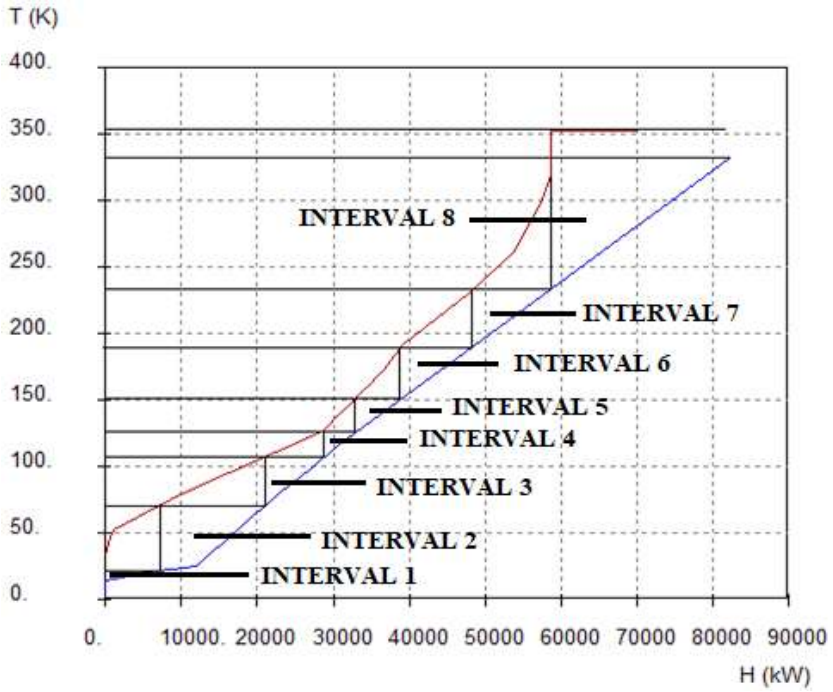


Figure 10. Balanced hot and cold composite curves, including utility contributions, partitioned into the eight enthalpy intervals used in the simplified superstructure procedure.

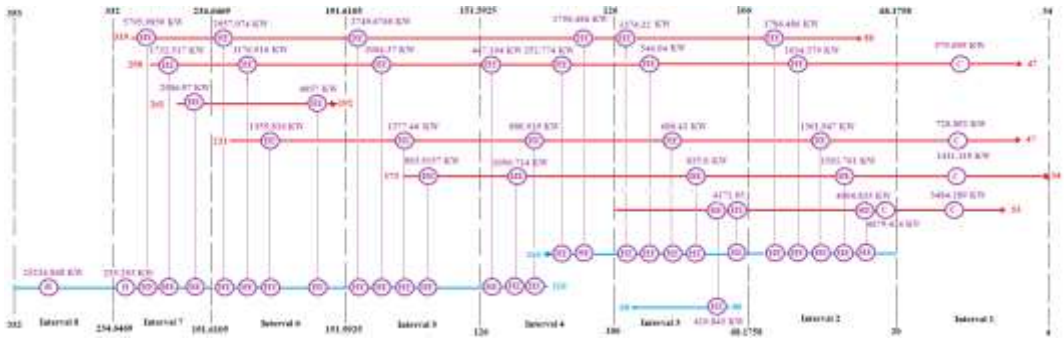


Figure 11. Complete HEN generated by the simplified superstructure approach before exchanger integration.

The integrated configuration is shown in Fig. 12. Counting the symbols in the figure gives 13 process exchangers, four coolers and one heater, i.e. 18 equipment units, in agreement with the reported total. The shell labels in the figure (nS-HE, nS-C, nS-H) sum to 34 (27 in process exchangers, 5 in coolers and 2 in the heater), equal to the pre-integration shell count, so integration as drawn consolidates matches into multi-shell units without changing the total number of shells. The annotated utility duties (approximately 23,460 kW for the heater and 10,880 kW for the four coolers) agree with the targets within 0.03%. Relative to the 14-unit minimum of Eq. (10), the 18-unit network contains four additional units, which corresponds to four independent loops or equivalent excess matches that could be candidates for loop breaking, at the cost of a larger temperature-driving-force penalty or a larger area on the remaining exchangers. The 34 shells exceed the 29-shell target by five (17%).

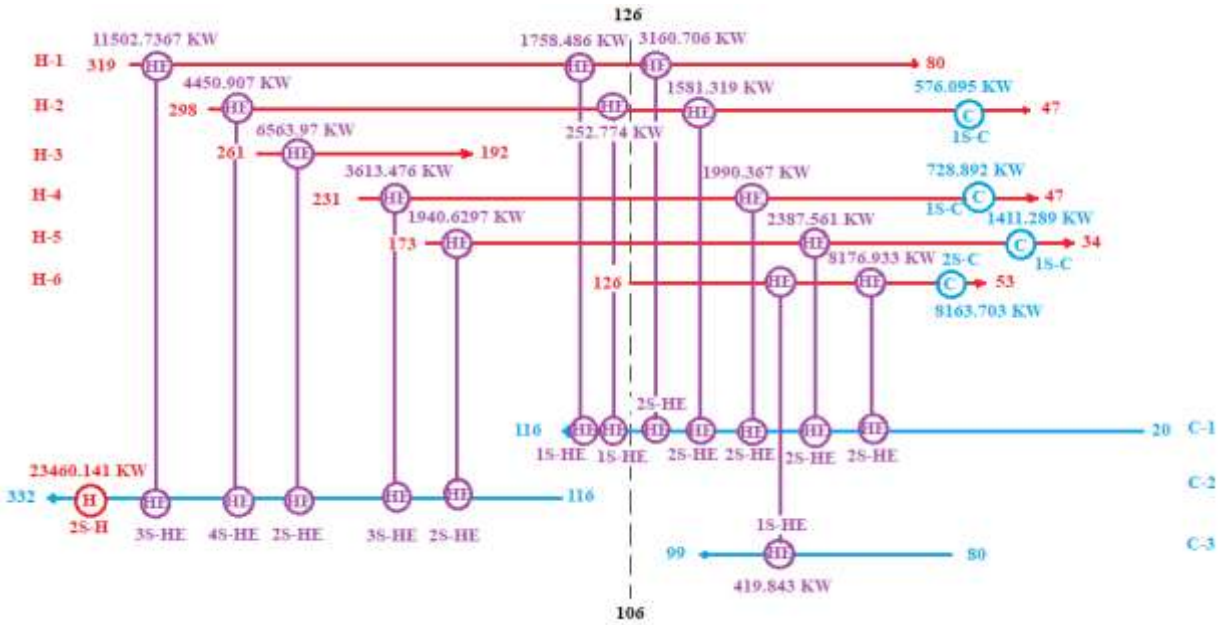


Figure 12. Integrated HEN obtained using the simplified superstructure approach (duties in kW; nS denotes the number of shells in each unit).

4.5. Cross-method comparison

Table 6 collects the reported design metrics. The values describe different quantities and are not interchangeable: 29 is a shell target, 14 and 18 are equipment-unit counts, and 34 is a shell count. Table 7 contrasts the two approaches qualitatively.

Table 6. Comparison of the reported pinch-based and simplified-superstructure design results, distinguishing shell targets and counts from equipment-unit counts.

Design result	Metric	Value	Breakdown/interpretation
Shell target (balanced composite curves)	Shells	29	13 below + 16 above pinch (28.1097 before rounding)
Pinch-based network	Equipment units	14	9 process exchangers + 1 heater + 4 coolers; equals $U_{min,MER}$
Simplified superstructure, before integration	Shells	34	17% above the shell target
Simplified superstructure, integrated	Equipment units	18	13 process exchangers + 1 heater + 4 coolers (34 shells in total)

Table 7. Qualitative comparison of the pinch-based design and the simplified superstructure approach for the Zawiya unit.

Aspect	Pinch-based design	Simplified superstructure
Primary role	Energy targets and design rules for network topology	Interval-wise generation of candidate matches and network construction
Utility duties	Equal the targets (23,457.156 and 10,882.814 kW)	Within 0.03% of the targets (as annotated in Fig. 12)
Equipment units	14, equal to $U_{min,MER}$	18, four above $U_{min,MER}$
Shells	Not reported for the network	34 versus a target of 29
Main strength	Transparent rules; minimum units without loops	Systematic, interval-wise accounting that supports shell-based evaluation
Main limitation here	No area or cost data for the network	Excess units that require loop breaking; judgement in interval partitioning

The comparison confirms the complementary roles of the two approaches. Pinch analysis fixes the thermodynamic targets (Table 2) and, through the no-cross-pinch rules, yields a network that achieves both the utility targets and the minimum unit count. The simplified superstructure organises candidate matches by enthalpy interval and provides a framework for shell-based evaluation and exchanger integration, but, as drawn, it carries four more units than the minimum. These results do not establish that either network is smaller, cheaper or operationally superior overall, because the networks have not been evaluated on a common basis of heat-transfer area, capital and operating cost, or controllability.

4.6. Limitations and implications

Four limitations qualify the findings. First, the TAC curve underlying ΔT_{min} = 20 °C cannot be reproduced independently because the annualisation period, utility prices, area-cost correlation, installation factors and operating hours are not itemised; the optimum should be tested for sensitivity to these inputs, particularly the relative cost of fuel and exchanger area. Second, exchanger areas, design conditions and the interval-wise match schedule of the superstructure network are not reported, so shell counts cannot be converted into area or cost. Third, the shell target depends on the adopted loading factor of 0.85 in Eq. (6) and on the representation of the hot utility as a 1 °C stream (Section 4.2). Fourth, the 374 kW difference in hot-utility target relative to Rahouma et al. [3] can be resolved only by comparing the underlying stream data.

For practical application, the networks should be assessed against constraints that targeting does not capture, including the crude temperature required at the desalter, fouling in the crude-preheat exchangers, available plot space, controllability and the topology of the existing exchangers. The reported results are therefore best regarded as a thermodynamic and structural benchmark that supports a subsequent economic and retrofit study.

5. Conclusions

This study compared pinch-based HEN design with a simplified superstructure approach for the crude-oil atmospheric distillation unit at Zawiya Refinery. The main findings are as follows.

(1) The HINT TAC curve has its minimum at ΔT_{min} = 20 °C, at which the minimum hot- and cold-utility targets are 23,457.156 kW and 10,882.814 kW, with pinch temperatures of 126 °C (hot) and 106 °C (cold). The maximum process-to-process recovery is 47,800 kW, 81.5% of the hot-stream duty.

(2) The hot-utility target is 374 kW (1.6%) below the value reported by Rahouma et al. [3]. Because the cold-utility targets agree, the net heat deficits of the two data sets differ by 374 kW, which indicates a difference in stream data rather than in ΔT_{min}.

(3) Shell targeting on the balanced composite curves gives 28.1097 shells before rounding (12.5642 below and 15.5455 above the pinch) and a target of 29 shells after separate upward rounding. The calculation is fully defined by Eqs. (2)–(9) with a $0.85P_{max}$ loading criterion.

(4) The pinch-based network comprises nine process exchangers, one heater and four coolers (14 units). It equals the minimum number of units for maximum energy recovery and meets both utility targets.

(5) The simplified superstructure uses eight enthalpy intervals and requires 34 shells before integration; its integrated network contains 18 units (13 process exchangers, one heater, four coolers), four more than the minimum.

(6) Pinch analysis and the simplified superstructure are complementary: the former establishes energy targets and design constraints, the latter supports interval-wise network construction. No economic or operational ranking can be made until heat-transfer area, capital and operating cost, and operability are evaluated on a common basis.

Future work should (i) report the TAC model and reconcile the stream data with Rahouma et al. [3]; (ii) add area targeting and detailed exchanger design for both networks; (iii) break the loops in the superstructure network and quantify the resulting trade-off; and (iv) assess the retrofit of the existing exchangers with fouling and operability constraints.

References

[1] Ballut, A.A., 1986. Heat recovery analysis of an existing crude distillation unit. *Heat Recovery Systems* 6 (5), 361–367.

[2] Alzanaty, K.A., 2009. Optimization using pinch technology. Operating manual of distillation of the Zawia Oil Refining Plant. Master's thesis, Libya.

[3] Rahouma, A.A., Krir, N.A., Abduallah, A.B., 2022. Optimizing design of heat exchanger network grassroots for crude oil distillation unit at Zawia Oil Refining Plant. *International Science and Technology Journal* 31, 1–17.

[4] Furman, K.C., Sahinidis, N.V., 2002. A critical review and annotated bibliography for heat exchanger network synthesis in the 20th century. *Industrial & Engineering Chemistry Research* 41 (10), 2335–2370.

[5] Klemeš, J.J., Kravanja, Z., 2013. Forty years of heat integration: pinch analysis (PA) and mathematical programming (MP). *Current Opinion in Chemical Engineering* 2 (4), 461–474.

[6] Linnhoff, B., Flower, J.R., 1978. Synthesis of heat exchanger networks: I. Systematic generation of energy optimal networks. *AIChE Journal* 24 (4), 633–642.

[7] Linnhoff, B., Hindmarsh, E., 1983. The pinch design method for heat exchanger networks. *Chemical Engineering Science* 38 (5), 745–763.

[8] Kemp, I.C., 2007. *Pinch Analysis and Process Integration: A User Guide on Process Integration for the Efficient Use of Energy*, 2nd ed. Butterworth-Heinemann (Elsevier), Oxford.

[9] Smith, R., 2016. *Chemical Process Design and Integration*, 2nd ed. John Wiley & Sons, Chichester.

[10] Papoulias, S.A., Grossmann, I.E., 1983. A structural optimization approach in process synthesis—II: Heat recovery networks. *Computers & Chemical Engineering* 7 (6), 707–721.

[11] Yee, T.F., Grossmann, I.E., 1990. Simultaneous optimization models for heat integration—II. Heat exchanger network synthesis. *Computers & Chemical Engineering* 14 (10), 1165–1184.

[12] Lewin, D.R., 1998. A generalized method for HEN synthesis using stochastic optimization. *Computers & Chemical Engineering* 22 (10), 1387–1405.

[13] Ponce-Ortega, J.M., Serna-González, M., Jiménez-Gutiérrez, A., 2009. Use of genetic algorithms for the optimal design of shell-and-tube heat exchangers. *Applied Thermal Engineering* 29 (2–3), 203–209.

[14] Bejan, A., Tsatsaronis, G., Moran, M., 1996. *Thermal Design and Optimization*. John Wiley & Sons, New York.

[15] Asante, N.D.K., Zhu, X.X., 1997. An automated and interactive approach for heat exchanger network retrofit. *Chemical Engineering Research and Design* 75 (A3), 349–360. https://doi.org/10.1205/026387697523660

[16] Ahmad, S., Linnhoff, B., Smith, R., 1990. Cost optimum heat exchanger networks—2. Targets and design for detailed capital cost models. *Computers & Chemical Engineering* 14 (7), 751–767.